Ji et al. Urban Informatics (2024) 3:4
https://doi.org/10.1007/s44212-023-00031-7

Urban Informatics

ORIGINAL ARTICLE

Open Access

An urban-scale spatiotemporal optimization of rooftop photovoltaic charging of electric vehicles

Nanfan Ji[1], Rui Zhu[2*], Ziyi Huang[1] and Linlin You[3]

Abstract

Solar photovoltaic (PV) farming is increasingly being used to power electric vehicles (EVs). Although many studies have developed dynamic EV charging prediction and scheduling models, few of them have coupled rooftop PV electricity generation with the spatiotemporal EV charging demands at an urban scale. Thus, this study develops a research framework containing three interconnected modules to investigate the feasibility of EV charging powered by rooftop PVs. The framework is constructed by the statistics of time serial EV charging demands at each station, the planning of rooftop PV installations associated with all charging stations, and the development of a dynamic dispatching algorithm to transmit surplus electricity from one station to another. The algorithm can maximize the overall balance between supply and demand, maximize the total PV electricity generation while minimising the total PV area, minimize the number of PV charging stations used as the suppliers for dynamic dispatch, and minimize the total electricity transmission distance between stations given the same power supply. The experiment utilizes a complete EV charging dataset containing 5574 charging piles with more than 9.7 million records in June and July in Guangzhou, China. The results show that rooftop PVs can supply more than 90% of the charging demand. The results encourage and inspire us to generalize and promote such a solution in other cities. Future work can refine the algorithm by adapting different PV sizes into various charging stations to further improve the electricity generation capability and the dynamic dispatching efficiency.

Keywords GIScience, Solar energy, Photovoltaic potential estimation, Electric vehicles, Multi-objective optimization, Dynamic dispatching

1 Introduction

1.1 Background

Excessive carbon emissions can cause global climate change, such as natural disasters and global warming (Shi & Yin, 2021). To reduce the total emission of greenhouse gases and alleviate global warming, many countries have successively committed to carbon neutrality (Liu et al., 2022). For instance, China contributed the largest CO_2 emission (31%) in 2021, exceeding the total value of CO_2 emissions of the US and the EU27, and the annual carbon emissions exceed 1 billion tons in China by 2022 (Friedlingstein et al., 2022). Meanwhile, the Chinese government strives to achieve carbon neutrality by 2060 (Wang et al., 2023). In this context, it is imperative to

*Correspondence:
Rui Zhu
zhur@ihpc.a-star.edu.sg
[1] Department of Land Surveying and Geo-Informatics, The Hong Kong Polytechnic University, 181 Chatham Road South, Kowloon, Hong Kong, China
[2] Institute of High Performance Computing (IHPC), Agency for Science, Technology and Research (A*STAR), 1 Fusionopolis Way, Singapore 138632, Republic of Singapore
[3] School of Intelligent Systems Engineering, Sun Yat-Sen University, Shenzhen 518107, China

shift energy supply from traditional fossil fuels to sustainable energy to address the issues caused by greenhouse gas emissions, such as global warming (McCarthy et al., 2010), air pollution (Zhang et al., 2023), and the heat island effect (Masson et al., 2014).

Solar photovoltaic (PV) systems with decreasing manufacturing costs have been recognized as a promising technology to decarbonize the power sector and are estimated to meet 25%–49% of global electricity demand by 2050 (He et al., 2020; Huang et al., 2019). Many PV systems have been deployed in grid-connected and off-grid systems in recent years (Das et al., 2018), which takes an advantage of easier operation in terms of power generation and can be used in both stand-alone systems and grid-connected applications (Charfi et al., 2018). Meanwhile, electric vehicles (EVs) with a growing global share alleviate the urgent energy crisis and environmental degradation (Papoutsoglou et al., 2022; Schmeck et al., 2022). The utilization of EVs as an attractive alternative to traditional internal combustion engine-based cars takes advantage of less greenhouse gas emissions (Khwaja et al., 2021). For instance, China currently has about 496,000 public EV charging stations and about 678,000 private EV charging stations (Alphonse et al., 2022). However, the advantages of EVs would be greatly diminished if the EV charging station uses traditional fossil fuels as the electricity supply. In addition, proliferating EV charging demand will increase the grid's load, especially during peak hours of electricity consumption. Some studies investigated the prediction of real-time EV charging demand by utilizing machine learning methods to intergrate massive and heterogeneous spatio-temporal data (You et al., 2019; Chen et al., 2022).

Distributed PV systems with a synergistic advantage can tackle the above problems (Denholm et al., 2013; Nunes et al., 2015). For example, rooftop PVs (RPVs) can be used to power EV charging stations, which can reduce long-distance transmission losses of electricity and can therefore improve economic efficiency (Zhu et al., 2023). However, the electricity generation of RPVs fluctuates and has obvious heterogeneity over time and space due to the comprehensive effects of cloud cover (Wong et al., 2016), urban morphology (Zhu et al., 2020), and solar irradiation (Catita et al., 2014), which causes uncertainty in the power supply of EV charging stations. Therefore, it is imperative to accurately estimate RPV potential and develop a dynamic electricity dispatching method between nearby charging stations to improve the EV charging efficiency and try to meet the total EV charging demand, with an optimization of PV area planning.

1.2 Solar irradiation estimation

Accurate estimation of solar PV potential near charging stations is crucial for integrating efficient solar charging potential into dynamic EV charging networks. The distribution of solar energy is influenced by urban morphology (Charfi et al., 2018) and meteorological conditions (Wong et al., 2016). Solar irradiation estimation considering three-dimensional (3D) urban surfaces can improve accuracy by considering the shading effects of buildings, trees, and other obstacles in the surrounding environment, or estimating the solar irradiation on the façade of buildings (Cheng et al., 2018; Gooding et al., 2015). In this regard, a 3D solar city model is built to observe solar accessibility in developing cities (Zhu et al., 2019). This model assists architects in urban planning by allowing solar radiation to illuminate the surface of the 3D city model to obtain a 3D building shadow surface and then evaluate the effects of new buildings on the PV potential of the surrounding buildings. Further study developed a spatio-temporal analysis model and a techno-economic evaluation model to optimize the PV supply (Zhu et al., 2022a). The study plans PV installation locations based on the solar irradiation estimation on 3D urban surfaces, which also indicates that the above two models are highly influenced by the quality of the 3D building model. This suggests that an integration of solar estimation model and high quality of 3D building model can result in a reliable solar distribution estimation. Therefore, it is appropriate to utilize the aforementioned models to estimate solar irradiation distribution for analysing the feasibility of EV charging powered by RPVs, since they can quantify the effects of the transmissivity, diffuse proportion, and the urban morphology.

1.3 Spatiotemporal dispatching of the generated electricity

Here, the dispatching refers to the transmission of electricity generated by RPVs to nearby charging stations to enhance the capacity of EV charging in a dynamic scenario. To solve the challenges of EV charging/discharging, one study proposed a management strategy based on the grid and a large charging station equipped with an energy storage system and PV modules that operated the power assignment (Li et al., 2020). Another study developed a methodology based on the micro-grid and electric vehicles cooperate optimization to solve for the desired system reliability given uncertainties in the power load and solar power supply (Ersal et al., 2013). The energy system of EV charging based on PV for the micro-grid in the industrial park mainly solves the problem of charging optimization scheduling of electric vehicles participating in the micro-grid. In comparison, some scholars focused on the low-carbon optimization strategy of power systems based on large-scale Vehicle-to-Grid (V2G) approach (Yao et al., 2022). The study constructed a "source-grid-vehicle" planning model based on traditional power generation, which optimized

the combination of different energy resources at a large scale. However, these studies did not develop a shareable network to dispatch the power between charging stations based on real-time power demand.

Further study developed a V2G network to balance power demand by using all parked EVs as a battery pool. The study assumed that all parked EVs are connected to the local V2G system in every district to aggregate as a large energy storage (Yu et al., 2016). However, it is impractical and cost consuming to apply to real charging stations due to uncontrollable uncertainty. Furthermore, Alqahtani & Hu (2020) proposed a mobile prosumer network based on vehicle routes and energy dispatching to address the spatial and temporal energy demand challenge. The vehicle is a mobile prosumer with distribute energy customer, while each building or infrastructure serves as a consumer. From this study, it can be observed that EVs can supply energy to each consumer according to their energy loads and solar irradiation, and request charging from the electric grid. However, the study assumed that each region operates independently, meaning that solar irradiation from one region cannot influence another one. Alternatively, Boström et al. (2021) promoted a pure PV-EV system, a nationwide energy system to provide energy, and used EVs as storage to balance the intermittency of PV (Wouters et al., 2015). However, the PV power supply can be a drastic difference throughout the year if the PVs are deployed in high-latitude locations. The study indicates a significant decline of PV power supply in winter due to relatively lower solar irradiation, which requires increasing PV area to meet the total charging demand and then results in overcapacity of electricity generation in the remaining seasons.

Other studies also used the charging and discharging of electric vehicles to solve the power fluctuation problem on the load side of the micro-grid (Gooding et al., 2015), established scheduling around the charging and discharging costs between electric vehicles and the grid (Yu et al., 2016), or matched energy sources in independent areas having smart grid (Alqahtani & Hu, 2020; Wouters et al., 2015). However, these studies mainly focused on large-scale research, having a limitation in considering spatiotemporal heterogeneity of electricity supply and demand (Yu et al., 2016; Alqahtani & Hu, 2020). Additionally, when grid connection is not utilized while energy storage is involved through the integration of V2G and PV systems, few of them addressed how to resolve the issue of overcapacity caused by an excessively large PV panel area within a given region (Boström et al., 2021). As a result, these system optimizations are applicable to urban-scale PV deployment planning in different cities based on their varying specific characteristics.

Overall, previous studies mainly investigated power matching between independent spaces based on mutual exclusion, or an entire region as a demand responsive system for overall power matching. Few studied the impact of spatiotemporally varying PV potential on the uncertainty and flexibility of EV charging demands, which is an unsolved challenge for penetrating solar energy into mobility with EVs. Therefore, this study aims to develop a framework to maximize the EV charging capability using RPVs, achieved by the development of a dynamic dispatching algorithm over time and space.

1.4 Contribution

This study has three major contributions. First, this study develops a parallel computing strategy for efficiently estimating fine-scale solar potential over a large geographical area. The strategy is splitting the entire area into several subareas with a predefined overlapping region to get rid of the marginal effects of shadow from surrounding buildings. This means that multiple cores of CPUs can be utilized, avoiding full usage of RAM and computing resources at a time. Second, this study assumes the RPVs in circular areas centred at the EV charging stations to generate electricity and considers power distribution of overlapping circular areas under the condition of high charging station density. The circular area can be determined by the power demand of the corresponding charging stations. Third, we develop a dynamic dispatching algorithm that can maximize the EV charging capability by balancing the charging demand of charging stations and the PV electricity generation at the urban scale. The algorithm addresses the gap in effectively powering EVs with a well planning of RPVs. The three innovations are integrated into a comprehensive framework that can be generalized and applied to other cities.

The following sections are organized as follows. Section 2 introduces some methodology utilized in this study. Section 3 describes the experimental materials, including the study area and dataset pre-processing. Section 4 contains experimental results and accompanying analyses. Section 5 presents discussion and conclusion.

2 Methodology

2.1 Research framework

This study proposes a research framework containing three interconnected modules for dispatching PV electricity to EV charging stations (Fig. 1). First, EV charging records in all piles of all charging stations are used to create spatio-temporal statistics of EV charging demands. Specifically, the daily EV charging demands of each charging station are aggregated by time-series. Second, RPV potential is estimated by using a well-established 3D solar estimation model, and circular areas centred at

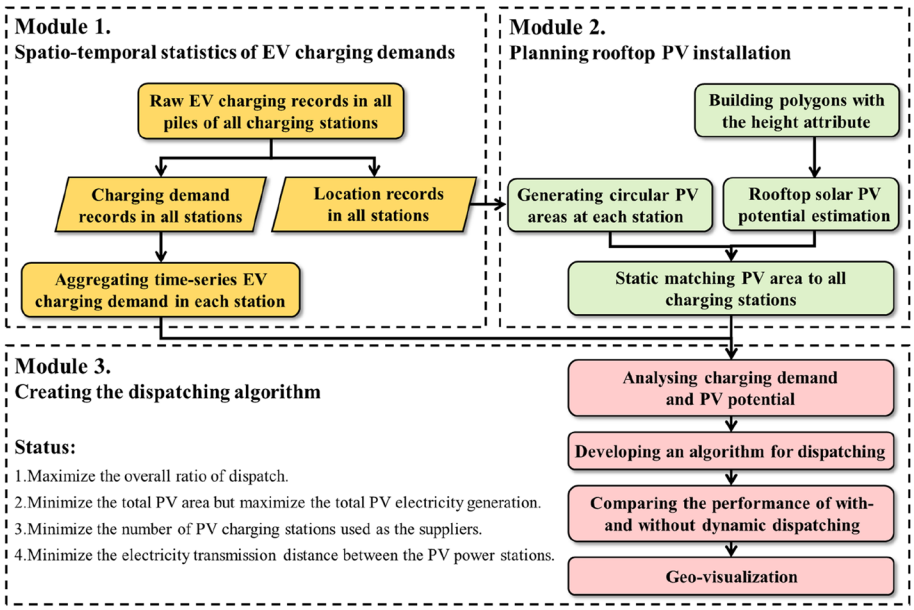

Fig. 1 Research framework

the EV charging stations are generated so that rooftops within the circular areas are assumed to be equipped with the PVs. After that, RPVs are matched to the corresponding charging stations, with the consideration of a complex scenario that two or more circular areas overlap with each other. Third, an optimization algorithm is developed to dynamically dispatch surplus electricity from one station to nearby ones having insufficient PV electricity generation. The performance of with- and without dynamic dispatching are compared to evaluate the effectiveness of the proposed algorithm, and geo-visualization enhances insights into solar PV distribution and dispatching performance.

2.2 Land surface solar irradiation estimation

The Area Solar Radiation toolset in ArcGIS Pro is used to estimate rooftop direct and diffuse solar irradiation, which can quantify the effects of geographic location (i.e., latitude and longitude), cloud cover determined by diffuse proportion and transmissivity, and shading effects from the surrounding 3D buildings (Zhu et al., 2022b). To reduce the solar potential uncertainty caused by unstable weather conditions, historical weather on the same day from 2009 to 2022 has been considered, which can be calculated by the proportion of clear days, partly cloudy days, and cloudy days to confidentially determine transmissivity (δ_t) and diffuse proportion (δ_d), as shown in Eqs. (1) and (2), respectively (Huang et al., 2008). Specifically, clear days are defined as having an average cloud cover of 0 to 30%, while partly cloudy days and cloudy days have an average cloud cover of 30% to 70% and of 70% to 100%, respectively (Wong et al., 2016). The proportion of cloud cover will influence the final solar potential estimation. This study assumes that the PV conversion efficiency is 22% and the performance ratio is 80% (Polman et al., 2016), which are typical values in practice. As a result, 17.6% of the received solar irradiation will convert to electricity.

$$\delta_t = 0.70P_{clear} + 0.50P_{partly} + 0.30P_{cloudy} \quad (1)$$

$$\delta_d = 0.20P_{clear} + 0.45P_{partly} + 0.70P_{cloudy} \quad (2)$$

where P_{clear}, P_{partly}, and P_{cloudy} are the proportions of sunny days, partly cloudy days, and cloudy days in a month, respectively.

2.3 Solar potential distribution estimation

Since it is time and cost intensive to utilize a single CPU process to estimate solar distribution for the entire city at a fine spatial resolution (e.g., 1 m), an alternative is separating the entire study area into a set of rectangular subareas (e.g., homogenous fishnets as shown in Fig. 2) and compute the solar irradiation in each subarea individually. To mitigate the marginal effect, it is important to extend the side length of each subarea with an x-meter external buffer to ensure that the shadowing effect made by 3D buildings along the marginal area can be considered for the solar distribution estimation. After completing the solar irradiation estimations for all subareas, each external buffer area will be clipped, and each grid cell will be maintained and unified to demonstrate the solar irradiation for the whole city.

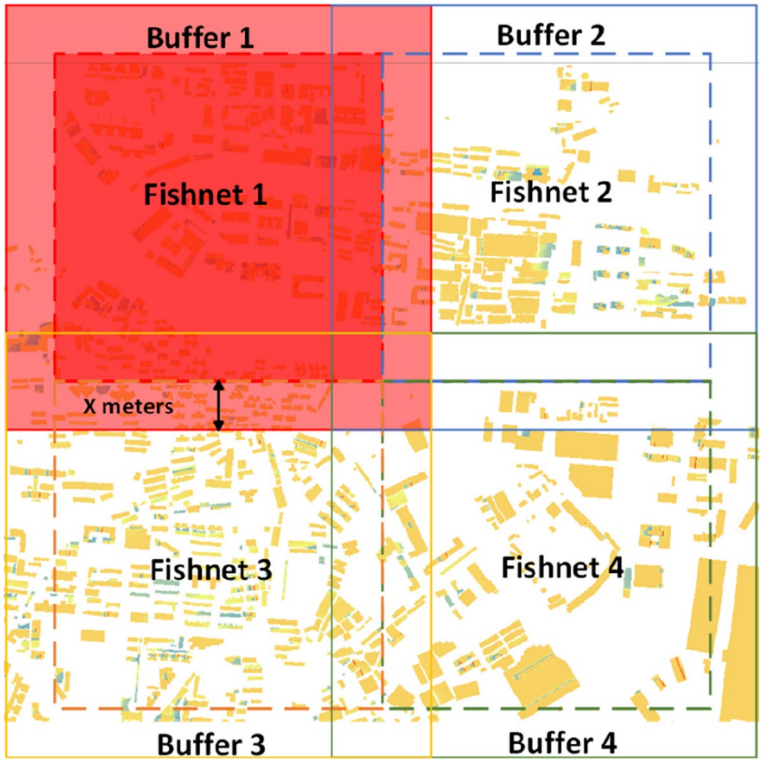

Fig. 2 Fishnet processing and extraction of solar irradiation

2.4 Spatio-temporal dynamic balancing between supply and demand

2.4.1 Static matching PV area to all charging stations

This study assumes that a circular area with an x-meter radius centralized at the location of the charging station will be used to plan RPVs to power this station and offset the electricity demand from the grid. PV modules will be deployed on the rooftops of the buildings in the circular area for PV electricity generation. Thus, the radius is a variable affecting the total installed capacity of the RPVs. When two or more charging stations are close enough, their circular areas are possible to overlap. In this case, the generated electricity in the overlapping area will be evenly distributed to the respective charging stations.

Figure 3 demonstrates the example of static matching PV areas to all charging stations, which has overlapped portions. Three charging stations are shown in blue, green, and yellow dots, respectively. Their external circular areas have overlapped areas as shown in orange and purple blocks, where the electricity generation of RPVs is evenly separated to the associated two charging stations. The RPVs covered in the remaining areas of the circles are the power supply to the corresponding charging station as shown in the blue, yellow, and green blocks, respectively. For economic considerations, areas with a PV potential less than 3 kWh/m^2/day will not be used to install PV modules (Cardoso et al., 2014).

2.4.2 Dynamic dispatching for charging stations

It is noticeable that the spatiotemporal charging demand and electricity supply are heterogeneous over time and space (Afridi, 2022). This means that the PV electricity generation to a single station may be insufficient or surplus, and dynamic dispatching of electricity between stations can effectively improve the PV charging efficiency of the entire electrical system, which is essentially a multi-objective optimization problem (Elma, 2020). The multi-objective optimization in this study has two tasks: the first one is the overall electricity balance, while the second one is the optimization of the total PV area. From a system-operation perspective, daily based dispatching is a practical solution.

In previous studies, the algorithms have employed various criteria such as maximizing economic benefits of solar PV energy (Cardoso et al., 2014), achieving peak load balancing after PV grid integration (Alqahtani & Hu, 2020; Yang et al., 2015), and rewarding different user charging behaviours under PV electricity self-consumption (Li et al., 2021). In comparison, our study focuses on spatial and dynamic optimization of EV charging based on solar PV potential. Therefore, the objectives of dynamic dispatching are to: (i) maximize the overall balance between supply and demand, which can be evaluated by the ratio of overall electricity supply to demand

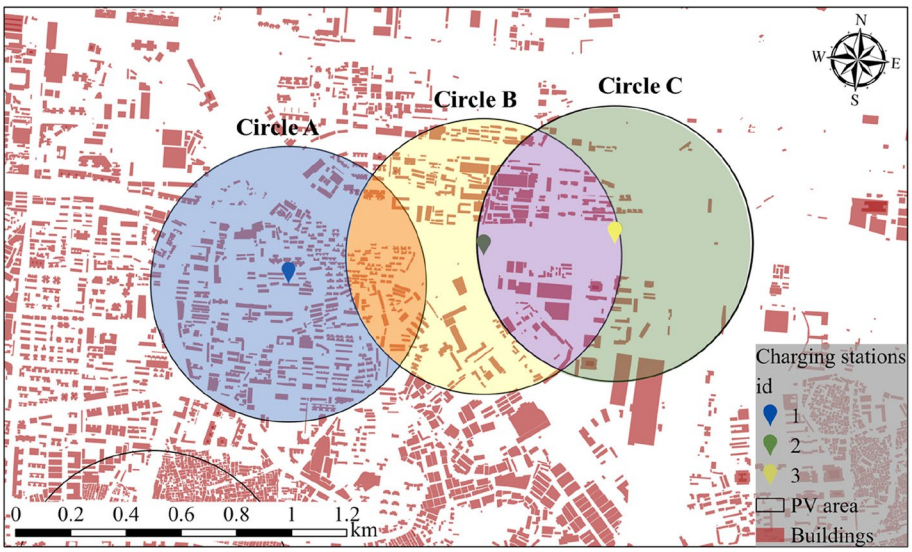

Fig. 3 The example of static matching PV area to all charging stations

aiming to reach 100%; (ii) minimize the total PV area but maximize the total PV electricity generation, which seeks for as small areas as possible to meet EV charging demand and avoid additional PV capacity at an urban scale; (iii) minimize the number of PV charging stations used as the suppliers for dynamic dispatch; and (iv) minimize the total electricity transmission distance of the PV power station under the condition of the same power supply. These four objectives comprehensively consider the facts that RPVs have significant spatial and temporal heterogeneity, and that electricity generation is influenced by different locations and time periods. Specifically, objective (i) aims to maintain the overall balance of RPV in time and space, while objective (ii) attempts to minimize the RPV electricity to reduce the production cost. Objectives (iii) and (iv) seek for complexity reduction of the entire dispatch system.

In this study, R represents the ratio of power supply to power demand of each charging station to differentiate the electricity provider (ep) and the electricity receiver (er). Thus, if R is less than one, the generated electricity associated with the charging station cannot meet its power demand. As the result, this charging station is defined as *er*. While R is greater than one, the corresponding charging station is defined as *ep*. Let MD be a dataset to record the successful dispatching. For $\forall er \in MD$, $\mathrm{er} = \{r_{id}, r_x, r_y, p_{id}, p_x, p_y\}$. It demonstrates that an electricity receiver is identified by the ID r_{id} and its longitude and latitude (r_x, r_y). Similarly, an electricity provider is identified by the ID p_{id} and its longitude and latitude (p_x, p_y). On this basis, three reasonable constraints set for dynamic dispatching as follows:

1. The power of the target ep participating in power dispatch should be greater than its demand power to contribute electricity to er, quantified by Eqs. (3) and (4) as follows:

$$f(ep) = e_{sply}(ep) - e_{dmd}(er) \quad \forall er \in ER, ep \in EP \tag{3}$$

$$\frac{f(ep)}{e_{dmd}(ep)} \geq 1 \tag{4}$$

where $e_{sply}(ep)$ represents the total electricity generated by ep, while $e_{dmd}(er)$ is the required additional power of er in the power dispatch. After dispatching, $f(ep)$ is the remaining electricity of ep. Equation (4) limits ep to satisfy its own demand first.

2. When there are several electricity providers that can supply the same amount of electricity, the dispatching will choose the one with the shortest electricity transmission distance between charging stations. The distance between charging stations is calculated according to their locations, using the Haversine formula (Andreou et al., 2023) as shown in Eqs. (5), (6), and (7) as follows:

$$dis(1,2) = 2arcsin\sqrt{sin^2\frac{a}{2} + \cos(\varphi_1) \times \cos(\varphi_2) \times sin^2\frac{b}{2}} \times r \quad (5)$$

$$a = \varphi_2 - \varphi_1 \quad (6)$$

$$b = \lambda_2 - \lambda_1 \quad (7)$$

where φ_1, φ_2 represent the latitude of point 1 and point 2, and λ_1, λ_2 correspond to the longitude of point 1 and point 2, while r refers to the radius of the sphere.

3. If the electricity from electricity providers is the same, then the transmission distance should be minimized, as presented in Eq. (8).

$$Min\, dis(er, ep) \quad \forall\, er \in ER, ep \in EP \quad (8)$$

where $Min\, dis(er, ep)$ means that the minimized transmission distance between *er* and *ep*.

Based on the above constraints, the algorithm is presented in a flow chart (Fig. 4) with the following steps.

1. The first step is to find out all the charging stations with $R < 1$ and identify them as electricity receivers so that a dataset named *ER* is created. For $\forall\, er \in ER$, $ER = \{id, lat, lon, e_d, ms\}$, an electricity receiver *er* is recorded by ID (*id*), latitude (*lat*), longitude (*lon*), the insufficient amount of electricity (e_d), and the binary matching status (*ms*).
2. The second step is to find out all charging stations that can meet the condition for every *er*. For $\forall\, er \in ER$, all the charging stations with $R \geq 1$, as demonstrated in Eq. (4), that located within 3 km to other electricity receivers will be defined as electricity providers. Meanwhile, a dataset named *EP* is created including the elements sorted in ascending order according to their surplus amount of electricity and sorted in descending order according to the distance between *ep* and *er*. The number of *ep* in the *EP* are marked as *N*. For $\forall\, ep \in EP$, $EP = \{id, lat, lon, e_s\}$, an electricity provider *ep* is recorded by ID (*id*), latitude (*lat*), longitude (*lon*), and the surplus amount of electricity (e_s).
3. The third step is to determine the conditional statement of *ep*.

    1) If there is no record in *EP*, which means no *ep* located within 3 km to other electricity receivers,

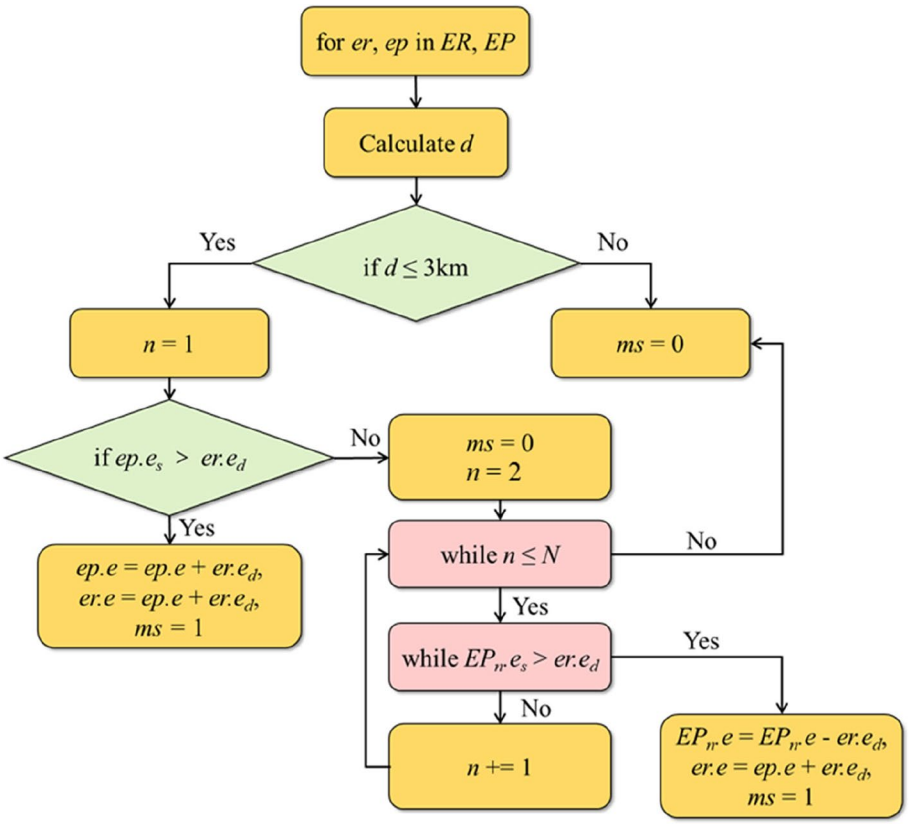

Fig. 4 Flow chart for dynamic dispatching algorithm

then the dispatch fails, and the *ms* will be marked as 0.

2) Otherwise, if there are records in *EP*, and because the reverse sorting is completed, the first record of *EP* which is the maximum *ep* must be the one with the highest power that can supply power to *er*. In this case, the dynamic dispatch of *er* and *ep* is one-to-one state. Consequently, the surplus amount of electricity of *ep* (e_s) will be compared with the insufficient amount of electricity of *er* (e_d):

   a) If $e_s > e_d$, which means the power supply of *ep* can satisfy the demand of *er*, then will update the remaining electricity of *EP* and mark the *ms* as 1.
   b) If $e_s < e_d$, which means that the power supply of *ep* cannot meet the demand of *er*, then multiple electricity providers will be used to dynamically dispatch a single *er*. It will select *n* electricity providers from the set *EP* sorted by row number at the beginning, marked as EP_n, and mark all the IDs of charging stations, updating the remaining electricity that *n* charging stations can provide, which is represents by $EP_n.e_s$; *n* is the number of charging stations which is less than or equal to *N*, the number of *EP* located within 3 km to other electricity receivers.
   c) If $EP_n.e_s > e_d$, then repeat step a). It should be noted that the update of the order of remaining electricity is the same as that of *EP*.
   d) If $EP_n.e_s < e_d$, then repeat step b) and step c) until *n* equals *N*.
   e) It is noted that if $n = N$ but the surplus amount of electricity $EP_n.e_s$ is still unsatisfied the insufficient amount of electricity e_d, then it will cancel the dispatch and mark *ms* as 0.

The pseudo code is presented to make a rigorous presentation (Table 1). In Lines 11–14, for each *er*, we calculate the distance (*d*) between *ep* and *er*, and select *ep* located within 3 km. If no station meets this condition, the status *ms* will be marked as 0. In Lines 15–19, we process one-to-one site dispatching if the surplus amount of electricity of *ep* ($ep.e_s$) satisfies the insufficient amount of electricity of *er* ($er.e_d$), and mark the status *ms* as 1 after successful dispatching. In Lines 20–30, if one-to-one site dispatching fails, we select a set of *n* selected electricity providers (EP_n) to execute multiple-to-one site dispatching and mark the status *ms* as 0 first. This step will be iterated until successful dispatching, and then mark status *ms* as 1. Lastly, in Lines 32–33, if dispatching still fails after finishing the iteration in step 3 or there is no *ep* located within 3 km to *er*, the status *ms* will be marked as 0.

As a local dispatching optimization algorithm, there are three obvious advantages: (i) in order to mitigate the issue of additional power loss brought on by the far-flung charging stations involved in the dispatch, dynamic power dispatch can be carried out through nearby charging stations; (ii) the ideal PV installation area size can be flexibly assessed based on the adjacent building density and the area's PV potential size; and (iii) residential units have autonomous energy systems. Therefore, even in places with unstable grids, nearby building units can be used to swiftly refuel charging stations with energy.

3 Empirical evaluation

3.1 Study area

Figure 5 demonstrates the study area, Guangzhou, China. It is reasonable to infer that charging demand will increase with the proliferation of EVs, either exponentially or linearly. To accelerate the EV charging station deployment, the Guangzhou Municipal Government has planned to build about 1000 super-fast charging stations and reach a total charging capacity of 4 million kilowatts by 2024. Meanwhile, the city has a variety of land use and land cover with complex urban morphology, which can create spatio-temporally heterogeneous RPV distribution. For instance, there are three typical industrial, commercial, and residential zones in the Huadu district, Tianhe district, and Liwan district, respectively. These three typical areas can help to easily understand the distribution of RPV at different times of the day. The selecting criteria refer to the density of the areas and the functional zoning of different areas. At the same time, 3D buildings are represented by raster data with a constant spatial resolution of 1 m. Therefore, the solar radiation of every single grid cell is finally determined to be 1×1 m^2.

3.2 Data pre-processing

The EV charging records were updated every five minutes for all the 476 charging stations in Guangzhou that corresponds to 5574 charging piles with a total number of more than 9.7 million records between 21 June and 20 July in 2022. Each record contains the attributes of station ID, latitude, longitude, power, charging status (no charging versus charging), charging mode (fast or slow charging), price, discounts, and charging duration. To quantify PV charging capability, the dataset is reconstructed to daily-based charging information through: (i) feature extraction: the charging rate and latitude–longitude features were extracted from each charging record, multiplied by the corresponding charging time to obtain the charging demand per minute; and (ii) data

Table 1 The pseudo codes of dispatching algorithm

```
Initialization
er: electricity receiver; ep: electricity provider
ER: {er}; EP: {ep}
N: the number of EP located within 3 km to other electricity receivers
n: the number of selected EP, n [1, N]
d: the distance between ep and er
e: the amount of electricity at a station
e_s: the surplus amount of electricity
e_d: the insufficient amount of electricity
ms: matching status
EP_n: a set of n selected EP, EP_n EP
Algorithm
for each er in ER
  for each ep in EP
    calculate d;
  if d ≤ 3 km
    n = 1;
    if ep.e_s > er.e_d
      ep.e = ep.e − er.e_d;
      er.e = er.e + er.e_d;
      ms = 1;
    else
      ms = 0;
      n = 2;
      while n ≤ N
        while EP_n.e_s > er.e_d
          EP_n.e = EP_n.e − er.e_d;
          er.e = er.e + er.e_d;
          ms = 1;
          break;
        if ms == 1
          break;
        n += 1;
  else
    ms = 0;
```

aggregation: each charging station was aggregated by ID, and the total daily charging demand and duration for each station were calculated.

The 3D building dataset was collected from the Institute of Geographic Sciences and Natural Resources Research, CAS, China. There are insignificant changes in solar irradiation in Guangzhou from June to July because the latitude of Guangzhou is 22°26' and the direct sunlight passes through Guangzhou twice by moving northward and turning southward at about 23°26' north latitude at the summer solstice around 22 June. Thus, this study performs bi-weekly estimations instead of calculating weekly or monthly average solar irradiation, as a trade-off between the accuracy and computation load. Meanwhile, it is important to incorporate the effects of unstable weather on RPV electricity generation. To estimate statistically significant RPV potential over the years, hourly cloud cover data in Guangzhou are collected for the past 14 years from 2009 to 2022 from World Weather Online (2023) and computed the average transmissivity and diffuse proportion for the two periods from 21 June to 5 July and from 6 to 20 July.

4 Results

4.1 Solar irradiation output

For administrative districts situated in the urban core, accounting for the impact of urban building patterns, particularly building height and density, as well as the urban RPV potential, an external buffer range x is established at 200 m to mitigate the above influences. Since the excessively low solar radiation is caused by the shadow effect from obstacles in the surrounding high-rise building, the areas with a PV potential less than 3 kWh/m^2/day are excluded to improve the efficiency and shorten the investment payback period (Luo et al., 2022; Wong et al., 2016). Although we only investigate solar potential on 28 June and 13 July, weather information is collected for the day before and the day after, for a total of three days, to minimize the influence of unstable weather. Table 2 lists the numbers and the average proportions of clear days, partly cloudy days, and cloudy days in the two short periods between 2009 and 2022. As a result, the transmissivity values on 28 June and 13 July in Guangzhou are 0.53 and 0.56, respectively, while the diffuse proportions are 0.41 and 0.37, respectively.

Table 3 shows the minimum and maximum values of solar irradiation in Guangzhou on 28 June and 13 July, respectively. It reveals that the highest values of solar irradiation occurred between 11:00 and 13:00 on both days, while the peak on July 13th is slightly higher than that on 28 June. Furthermore, the maximum value of solar irradiation gradually increased from 6:00 to 13:00, after that it slowly decreased. There is a reasonably sharp decline in maximum solar irradiation during the intervals from 16:00 to 18:00 with values of 314 Wh/m^2 on 28 June and 326 Wh/m^2 on 13 July, respectively.

Figure 6 visualizes the solar irradiation distribution from 6:00 to 18:00 in the industrial area in Huadu District, the commercial area in Tianhe District, and the residential area in Liwan District, which are the three typical areas corresponding to Fig. 5, respectively. It reveals that the commercial area had relatively low solar potential, especially from 7:00 to 8:00, which was mainly caused by the shadow effects from the high density of tall buildings. The visualization provides an explicit understanding of spatio-temporal changes in solar irradiation distribution

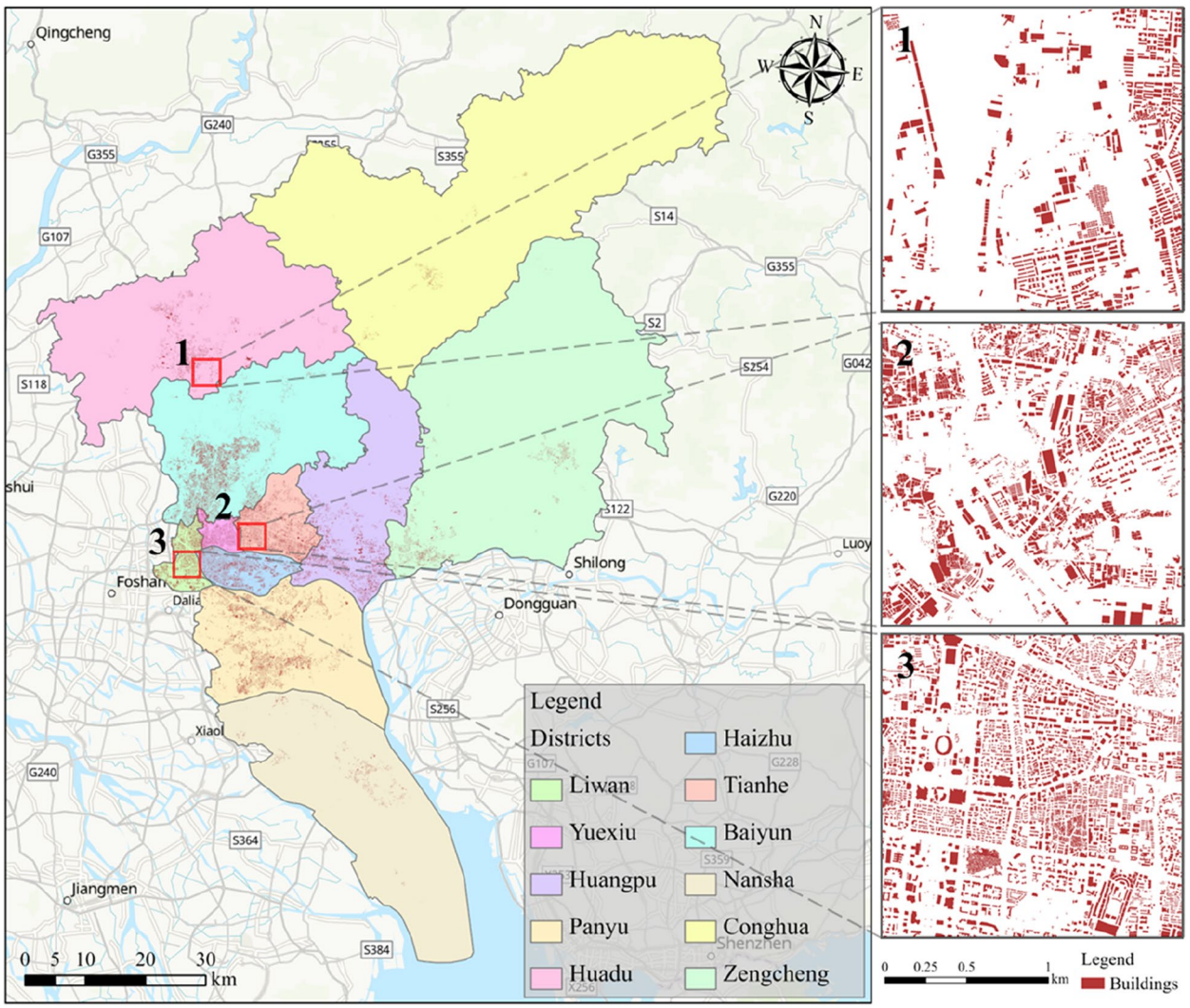

Fig. 5 Study area in the city of Guangzhou, China

during the daytime and assists in planning the deployment of RPV modules.

4.2 The supply–demand relationship without dispatching

Figure 7 demonstrates the proportion of three types of solar PV charging stations (in the y-axis) including completely satisfied ($R \geq 1$), partly satisfied ($R < 1$), and completely unsatisfied (W) according to the real EV charging demand and supply in different radius of circular PV area in the x-axis. As discussed in Sect. 2.4.2, R represents the electricity supply and demand ratio. Overall, the results are almost the same when the statistics are made for the first- and the second 15 days. It is noticeable that W equals 0.38 when the radius is 50 m, and with the increase of the radius to 500 m, W reduces to 0.09 (Fig. 7(a)). In the same scenario, the values are 0.17 and 0.02 for $R < 1$. In comparison, with the increase of the radius, the proportion of charging stations grow from 0.45 to 0.88 for $R \geq 1$, and the increasing trend turns to be rather slow since the radius reaches 250 m. This indicates that PV potential within a 250-m circular area might be a feasible choice since it has already been able to support more than 80% of the real charging demand without any dynamic balancing. The existence of W usually represents no appropriate building rooftops in this area, suggesting that a larger circular buffer area is required to generate the PV electricity. Figure 7(b) presents the similar trend and implications.

Figure 8 shows the supply–demand relationships without dispatching across the whole city for the first 15 days. Despite the high density of EV charging stations in Haizhu district and Tianhe district, the charging demand can be satisfied quickly with the increase in RPV areas compared with other administrative districts due to the

Table 2 The number of days in different types of climate information

	27–29 June 2009–2022	12–14 July 2009–2022
N_{clear}	10	14
N_{partly}	28	27
$N_{cloudly}$	4	1
P_{clear}	0.24	0.33
P_{partly}	0.67	0.64
$P_{cloudly}$	0.10	0.02
δ_t	0.53	0.56
δ_d	0.41	0.37

high density of buildings in these two districts as shown in Fig. 5. This means that there is a greater potential for RPV deployments in these areas within the same radius.

4.3 The supply–demand relationship with dispatching

The above section also reveals that the ratio for $R>1$ cannot reach 90% although the radius of the circular PV area has already been 500 m. This suggests that spatio-temporal dynamic dispatching may be an effective solution to further improve the PV charging capability at a given PV area. It is noticed that the dynamic dispatching is at the urban scale, which means that there are several different areas in the city, such as residential, industrial, and commercial areas, all utilized the dispatching system to address the imbalance between supply and demand of electricity. Thus, Fig. 6 shows the distribution of solar irradiation in different study areas, while the electricity dispatching system is used to balance the relationship between power supply and demand at the urban scale. Figure 9 depicts the proportion of two types of solar PV charging stations with dynamic dispatching. After dynamic dispatching, it is found that all charging stations can be powered by RPVs. For the two periods, the proportions of charging stations for $R\geq 1$ are around 10% to 20% larger than that without dynamic dispatching, versus the proportions of charging stations for $R<1$ are around 10% to 20% smaller. It has also been noticed that more than 90% of the charging stations can be completely powered by PVs with $R\geq 1$ when the PV planning area has a radius of 300 m. Since that, the improvement has become insignificant.

Figure 10 shows the supply–demand relationships with dispatching across the whole city. The electricity providers and receivers are represented by yellow and red dots in Fig. 10, respectively. It is found that the transmission of surplus electricity made by the proposed dynamic dispatching algorithm can satisfy the demand of adjacent charging stations with insufficient supply. However, the local supply–demand relationship remains unclear to be observed in Fig. 10. To demonstrate the effectiveness of the proposed framework, Fig. 11 demonstrates the local supply–demand relationship with dispatching in four specific areas including industrial, commercial, residential, and suburban areas. The number of charging stations that satisfy the demand or have the capability to provide power increases with the radius of the RPV areas. Meanwhile, the charging-demand relationship between different charging stations changes dynamically with increasing RPV areas. Finally, the insufficient power supply corresponding to the four areas has been solved by local dispatching with a radius of 250 m, 150 m, 100 m, and 400 m, respectively. It is uncompulsory to increase the radius to meet the charging demand of high-density charging stations as shown in the commercial

Table 3 Time series solar irradiation in Guangzhou on the two specific dates

Hour interval	28 June		13 July	
	Minimum (Wh/m^2)	Maximum (Wh/m^2)	Minimum (Wh/m^2)	Maximum (Wh/m^2)
6:00 – 7:00	0.00	168.78	0.00	187.08
7:00 – 8:00	0.01	484.14	0.01	513.23
8:00 – 9:00	0.01	703.91	0.01	730.60
9:00 – 10:00	0.01	839.92	0.01	863.39
10:00 – 11:00	0.01	928.88	0.01	939.06
11:00 – 12:00	0.01	1006.32	0.01	1016.95
12:00 – 13:00	0.02	1006.32	0.01	1016.95
13:00 – 14:00	0.01	928.88	0.01	939.06
14:00 – 15:00	0.01	839.54	0.01	863.05
15:00 – 16:00	0.01	704.21	0.01	730.87
16:00 – 17:00	0.01	484.34	0.01	513.42
17:00 – 18:00	0.00	170.33	0.00	187.98

Fig. 6 Hourly solar irradiation distribution from 6 am to 6 pm. **a** Industrial area. **b** Commercial area. **c** Residential area

zone (Fig. 11(b)). Specifically, the power supply highly depends on the building density and urban morphology instead of the type of functional zones. Overall, the dynamic dispatching algorithm can improve the charging capacity and minimize electricity waste.

Figure 12 presents the proportion of solar PV charging stations that were successfully dispatched (in the y-axis) on 28 June and 13 July, for different circular areas with the radius ranging from 50 to 500 m (in the x-axis). Overall, as the size of the PV planning area increases, the success ratio of dispatching charging stations tends to decrease, especially at high-capacity levels. However, there is an exception to this trend that, when the PV planning area has a 100-m radius, it obtains the highest rate of successful dispatching on both dates. This is probably because that when the PV size is significantly small (e.g., the radius is 50 m), the generated PV electricity can only be used for powering its own charging station, and there is surplus electricity that can be used for powering other charging stations when the PV size is getting bigger (e.g., the radius is 100 m).

5 Discussion and conclusion

This study proposed three interconnected modules for dispatching surplus electricity between EV charging stations to maximize the EV charging capability powered by RPVs. The developed algorithm achieved local optimizations that maximize the charging capacity, minimize

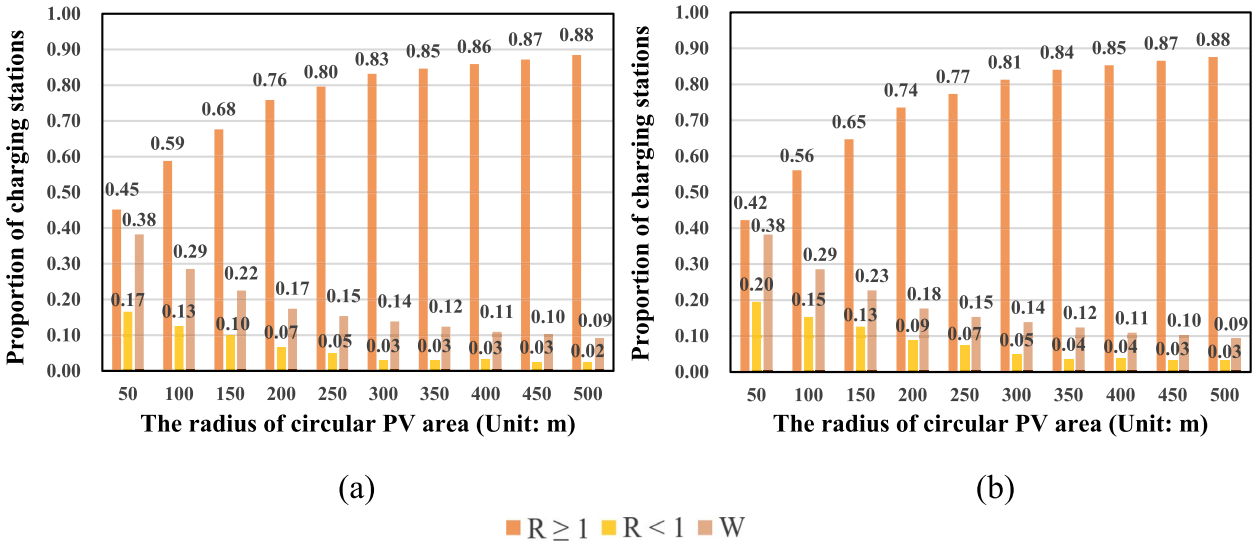

Fig. 7 The proportion of three types of solar PV charging stations without dispatching. **a** The statistics for the first 15 days. **b** The statistics for the second 15 days

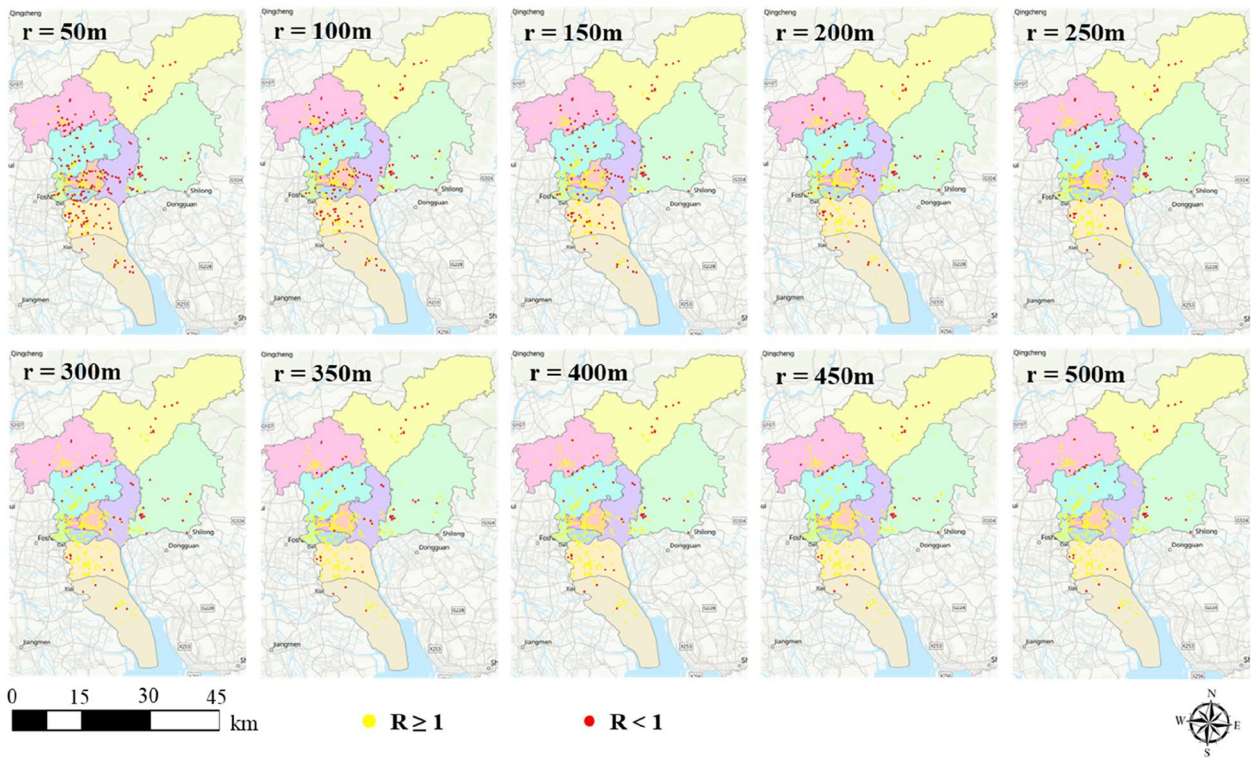

Fig. 8 The supply–demand relationship without dispatching for the first 15 days

the number of charging stations to be powered by other stations, and minimize the total power-transmission distance. The charging capacity increased by 20%, which is inspiring and encouraging us to promote such an approach in other cities with similar latitudes, building density, and urban morphology (e.g., Shenzhen and other cities in the Greater Bay Area of China). After collecting the data of diffuse proportion, transmissivity, and building attributes (i.e., locations and heights) for the 3D solar potential estimation model as well as the charging

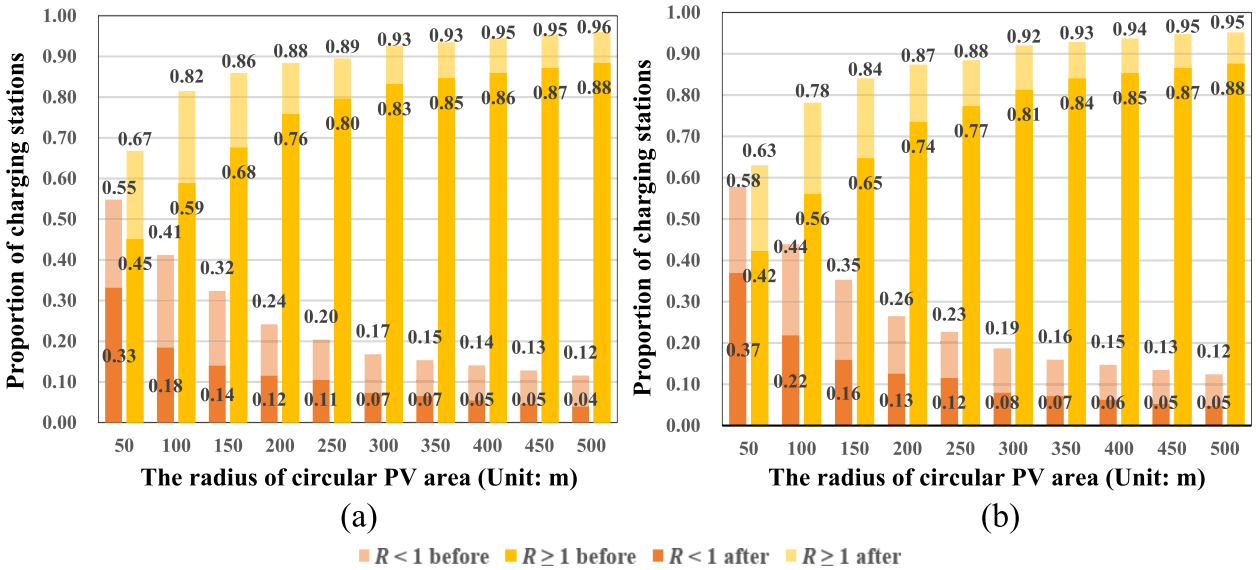

Fig. 9 The proportion of two types of solar PV charging stations with dispatching. **a** The statistics for the first 15 days. **b** The statistics for the second 15 days

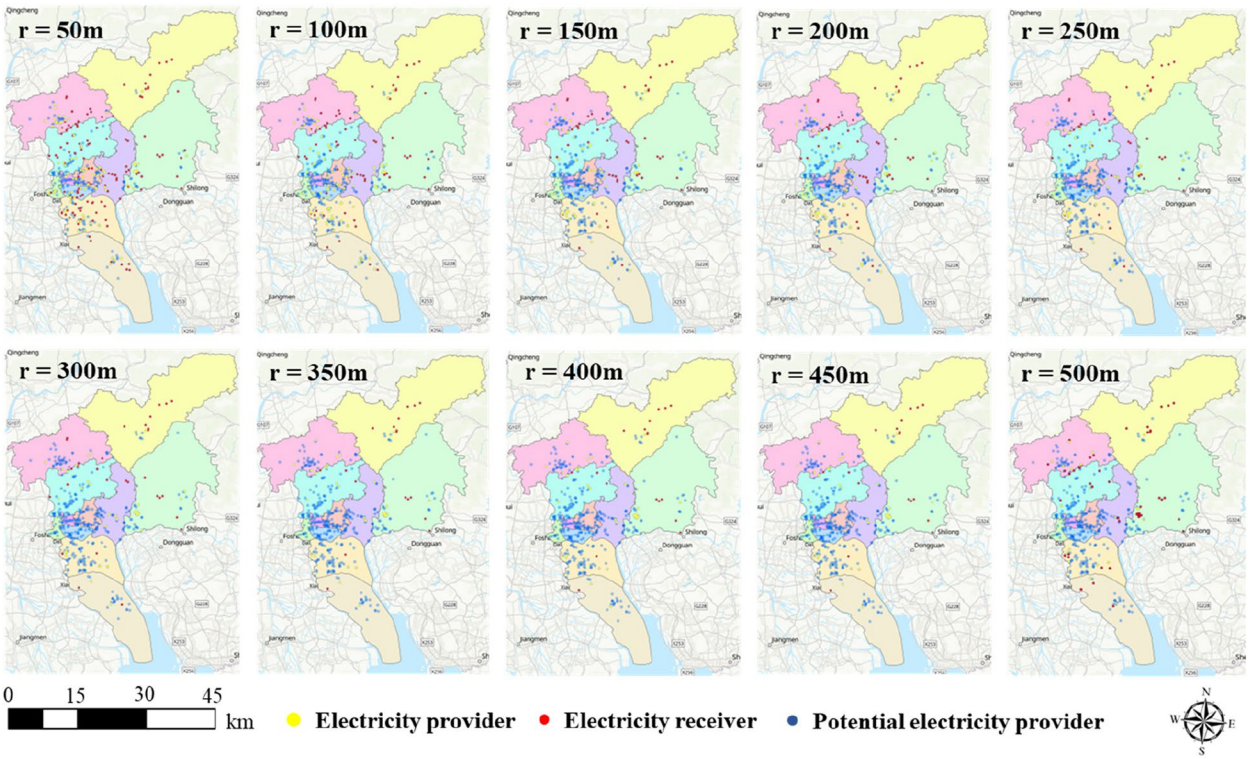

Fig. 10 The supply–demand relationship with dispatching for the first 15 days

demand and locations of EV charging stations, the appropriate radius of RPV areas can be obtained by utilizing this framework.

More types of functional areas might have little impact on the representative improvement of 3D solar potential estimation and dynamic dispatching optimization. This is because the estimation is determined by solar irradiation, building density, and urban morphology. Our study aims to find the appropriate radius of RPV areas to maintain the overall balance between supply and demand at the

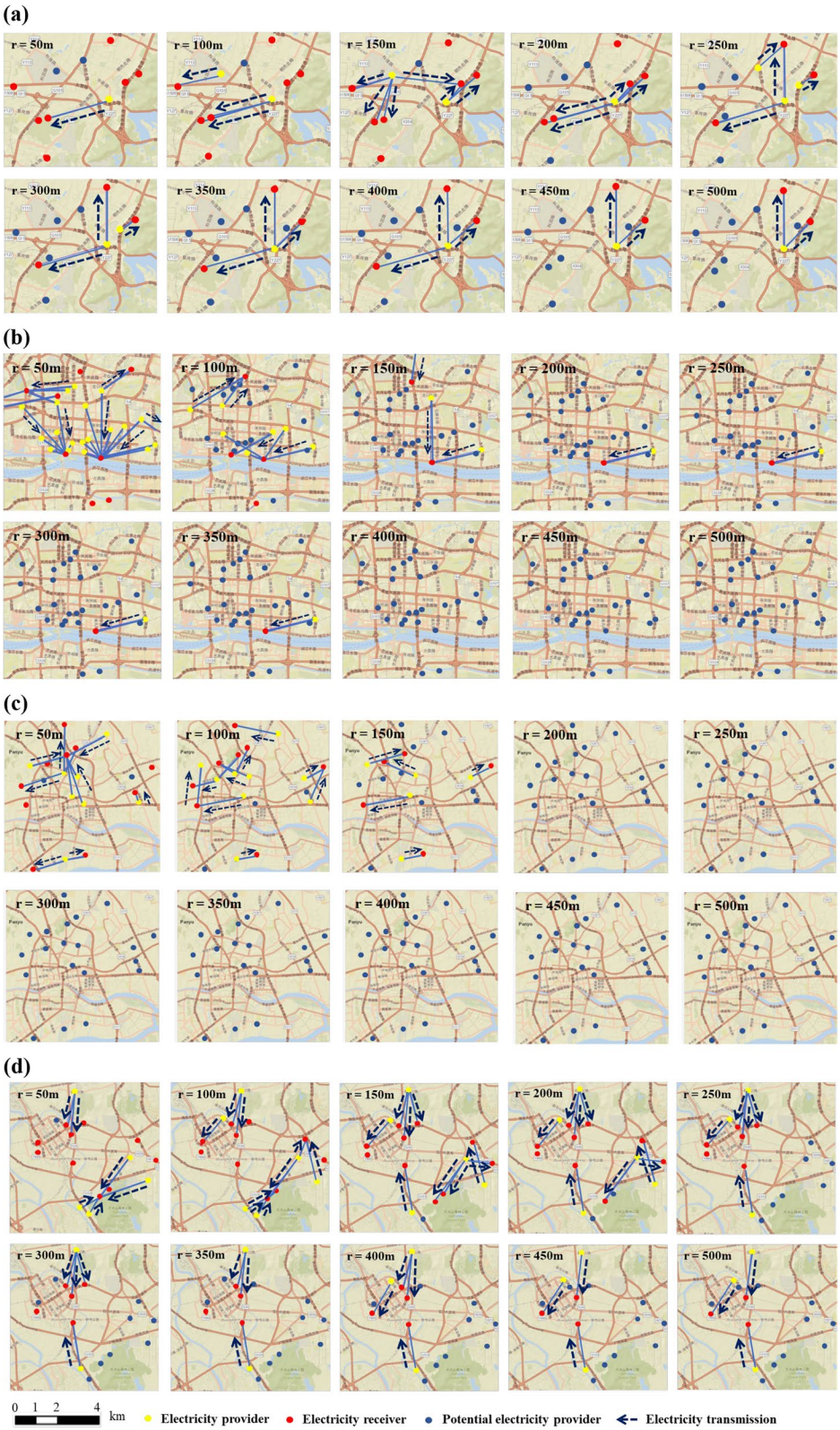

Fig. 11 The supply–demand relationship with dispatching in four specific areas for the first 15 days. **a** Industrial zone. **b** Commercial zone. **c** Residential zone. **d** Suburban area

urban scale. Meanwhile, the functional area distributions are complex within the city, and our study takes 3 km as the maximum transmission radius, which is large enough to cross different functional areas. Therefore, our study excludes the classification of functional areas in the section on estimating the 3D solar irradiation.

This study is vital in three aspects. First, we proposed a parallel computing strategy for efficiently estimating fine-scale solar potential over a large geographical area, which successfully reduce the computation time and computer performance requirements. Second, the developed algorithm contributes to spatiotemporal dispatching of RPV electricity for EV charging at an urban scale, which can dispense surplus power to minimize electricity waste. According to the pseudocode, the time complexity of this algorithm is $O(n^4)$, while the spatial complexity is $O(n^2)$. It is noticed that the time complexity is relatively large, which indicates that the execution time of a program increases exponentially with the amount of input data. Third, this study performed a series of experiments with varying sizes of PV planning areas, which was useful in suggesting the best one that can approach the balance between the power supply and demand between nearby charging stations. Notably, the RPV electricity generation between stations is also spatiotemporally heterogeneous. This is because rooftop solar potential was conclusively affected by rooftop areas and shadows created by 3D buildings of the same size as the circular planning area. In this regard, a flexible approach can integrate the optimization of varying radius of the PV planning area into the current model. Thus, our study is significant to accelerate the transition to sustainable power supply to reduce carbon emissions (long-term impact) and to reduce the grid load, especially in peak hours (short-term impact).

The solar estimation and PV planning made in this study were based on the horizontal rooftop surfaces that did not model rooftop structures and the affiliations. This can accurately quantify the theoretical solar PV potential but may cause certain uncertainty from reality. To solve this problem, building model reconstruction from 3D point clouds or rooftop semantic segmentation based on the high resolution of satellite imagery can be used for refined rooftop solar distribution estimation. Although the power loss due to electricity transmission was not counted, its impacts are insignificant and negligible since the transmission distance from providers and receivers is short enough.

To conclude, this study developed an urban-scale dynamic dispatching framework for powering EV charging stations with RPV electricity. The developed algorithm can be generalized and applied to other cities, demonstrating its practical significance in promoting sustainable urban development. This study also makes contributions to geographic science in revealing spatiotemporal patterns of solar distributions in cities. Future work can refine the dynamic dispatching algorithm by incorporating heterogeneous radius of the PV planning area, which can improve the PV electricity generation efficiency considerably.

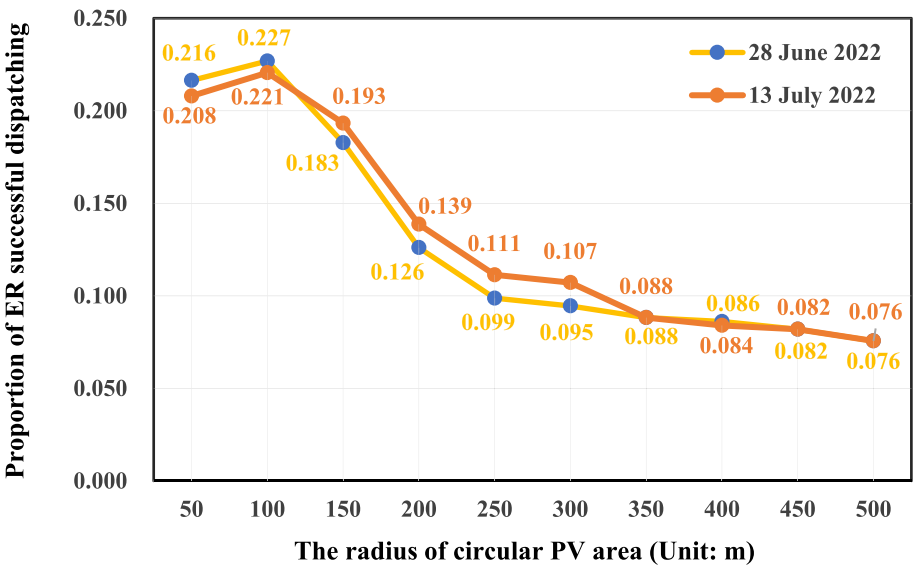

Fig. 12 The proportion of solar PV charging stations with successful dispatching for different circular areas

Acknowledgements
The authors would like to thank Haohao Qu and Qiyang Chen for data collection.

Authors' contributions
Conceptualization: Rui Zhu; Methodology: Nanfan Ji, Rui Zhu; Formal analysis and investigation: Nanfan Ji; Writing – original draft preparation: Nanfan Ji; Writing – review and editing: Rui Zhu, Ziyi Huang, Linlin You.

Funding
Not applicable.

Availability of data and materials
Data will be made available on request.

Declarations

Ethics approval and consent to participate
Not applicable.

Consent for publication
Not applicable.

Competing interests
The authors declare no conflict of interest.

Received: 13 August 2023 Revised: 8 November 2023 Accepted: 10 November 2023
Published online: 15 January 2024

References

Afridi, K. (2022). The future of electric vehicle charging infrastructure. *Nature Electronics, 5*(2), 62–64.
Alphonse, A. R. A., Raj, A. P. P. G., & Arumugam, M. (2022). Simultaneously allocating electric vehicle charging stations (EVCS) and photovoltaic (PV) energy resources in smart grid considering uncertainties: a hybrid technique. *International Journal of Energy Research, 46*(11), 14855–14876.
Alqahtani, M., & Hu, M. (2020). Integrated energy scheduling and routing for a network of mobile prosumers. *Energy, 200*, 117451.
Andreou, A., Mavromoustakis, C. X., Batalla, J. M., Markakis, E. K., Mastorakis, G., & Mumtaz, S. (2023). UAV trajectory optimisation in smart cities using modified a * algorithm combined with haversine and vincenty formulas. *IEEE Transactions on Vehicular Technology, 72*(8), 9757–9769.
Boström, T., Babar, B., Hansen, J. B., & Good, C. (2021). The pure PV-EV energy system – A conceptual study of a nationwide energy system based solely on photovoltaics and electric vehicles. *Smart Energy, 1*, 100001.
Cardoso, G., Stadler, M., Bozchalui, M. C., Sharma, R., Marnay, C., Barbosa-Póvoa, A., & Ferrão, P. (2014). Optimal investment and scheduling of distributed energy resources with uncertainty in electric vehicle driving schedules. *Energy, 64*, 17–30.
Catita, C., Redweik, P., Pereira, J., & Brito, M. (2014). Extending solar potential analysis in buildings to vertical facades. *Computers & Geosciences, 66*, 1–12.
Charfi, W., Chaabane, M., Mhiri, H., & Bournot, P. (2018). Performance evaluation of a solar photovoltaic system. *Energy Reports, 4*, 400–406.
Chen Q., Liu S., Qu H., Zhu R., & You L. (2022, December). TWAFR-GRU: An Integrated Model for Real-time Charging Station Occupancy Prediction, In *19th IEEE International Conference on Ubiquitous Intelligence and Computing* (pp. 1611-1618). IEEE.
Cheng, L., Xu, H., Li, S., Chen, Y., Zhang, F., & Li, M. (2018). Use of LiDAR for calculating solar irradiance on roofs and façades of buildings at city scale: Methodology, validation, and analysis. *ISPRS Journal of Photogrammetry and Remote Sensing, 138*, 12–29.
Das, U. K., Tey, K. S., Seyedmahmoudian, M., Mekhilef, S., Idris, M. Y. I., Deventer, W. V., Horan, B., & Stojcevski, A. (2018). Forecasting of photovoltaic power generation and model optimization: a review. *Renewable and Sustainable Energy Reviews, 81*, 912–928.
Denholm, P., Kuss, M., & Margolis, R. M. (2013). Co-benefits of large scale plug-in hybrid electric vehicle and solar PV deployment. *Journal of Power Sources, 236*, 350–356.
Elma, O. (2020). A dynamic charging strategy with hybrid fast charging station for electric vehicles. *Energy, 202*, 117680.
Ersal, T., Ahn, C., Peters, D. L., Whitefoot, J. W., Mechtenberg, A. R., Hiskens, I. A., Peng, H., Stefanopoulou, A. G., Papalambros, P. Y., & Stein, J. L. (2013). Coupling between component sizing and regulation capability in microgrids. *IEEE Transactions on Smart Grid, 4*(3), 1576–1585.
Friedlingstein, P., O'Sullivan, M., Jones, M. W., Andrew, R. M., Gregor, L., Hauck, J., Le Quéré, C., Luijkx, I. T., Olsen, A., Peters, G. P., Peters, W., Pongratz, J., Schwingshackl, C., Sitch, S., Canadell, J. G., Ciais, P., Jackson, R. B., Alin, S. R., Alkama, R., . . . Zheng, B. (2022). Global Carbon Budget 2022. *Earth System Science Data*, *14*(11), 4811–4900.
Gooding, J., Crook, R., & Tomlin, A. S. (2015). Modelling of roof geometries from low-resolution LiDAR data for city-scale solar energy applications using a neighbouring buildings method. *Applied Energy, 148*, 93–104.
He, G., Lin, J., Sifuentes, F., Liu, X., Abhyankar, N., & Phadke, A. (2020). Rapid cost decrease of renewables and storage accelerates the decarbonization of China's power system. *Nature Communications, 11*, 2486.
Huang, S., Rich, P. M., Crabtree, R. L., Potter, C. S., & Fu, P. (2008). Modeling monthly near-surface air temperature from solar radiation and lapse rate: application over complex terrain in yellowstone national park. *Physical Geography, 29*(2), 158–178.
Huang, Z., Mendis, T., & Xu, S. (2019). Urban solar utilization potential mapping via deep learning technology: a case study of Wuhan, China. *Applied Energy, 250*, 283–291.
Khwaja, A. S., Venkatesh, B., & Anpalagan, A. (2021). Performance analysis of LSTMs for daily individual EV charging behavior prediction. *IEEE Access, 9*, 154804–154814.
Li, D., Zouma, A., Liao, J. T., & Yang, H. Z. (2020). An energy management strategy with renewable energy and energy storage system for a large electric vehicle charging station. *eTransportation, 6*, 100076.
Li, S., Hu, W., Cao, D., Dragičević, T., Huang, Q., Chen, Z., & Blaabjerg, F. (2021). Electric vehicle charging management based on deep reinforcement learning. *Journal of Modern Power Systems and Clean Energy, 10*(3), 719–730.
Liu, Z., Deng, Z., Davis, S. J., Giron, C., & Ciais, P. (2022). Monitoring global carbon emissions in 2021. *Nature Reviews Earth & Environment, 3*(4), 217–219.
Luo, X., Pan, L., & Yang, J. (2022). Mineral resource constraints for China's clean energy development under carbon peaking and carbon neutrality targets: quantitative evaluation and scenario analysis. *Energies, 15*(19), 7029.
Masson, V., Bonhomme, M., Salagnac, J. L., Briottet, X., & Lemonsu, A. (2014). Solar panels reduce both global warming and urban heat island. *Frontiers in Environmental Science., 2*, 14.
McCarthy, M. P., Best, M. J., & Betts, R. A. (2010). Climate change in cities due to global warming and urban effects. *Geophysical Research Letters, 9*, 37.
Nunes, P., Farias, T., & Brito, M. C. (2015). Day charging electric vehicles with excess solar electricity for a sustainable energy system. *Energy, 80*, 263–274.
Papoutsoglou, M., Rigas, E. S., Kapitsaki, G. M., Angelis, L., & Wachs, J. (2022). Online labour market analytics for the green economy: the case of electric vehicles. *Technological Forecasting and Social Change, 177*, 121517.
Polman, A., Knight, M., Garnett, E. C., Ehrler, B., & Sinke, W. C. (2016). Photovoltaic materials: present efficiencies and future challenges. *Science, 352*(6283), 307–307.
Schmeck, H., Monti, A., & Hagenmeyer, V. (2022). Energy informatics: key elements for tomorrow's energy system. *Communications of the ACM, 65*(4), 58–63.
Shi, S., & Yin, J. (2021). Global research on carbon emissions: A scientometric review. *Environmental Impact Assessment Review, 89*, 106571.
Wang, Y., Wang, M., Teng, F., & Ji, Y. (2023). Remote sensing monitoring and analysis of Spatiotemporal changes in China's Anthropogenic carbon emissions based on XCO2 data. *Remote Sensing, 15*(12), 3207.
Wong, M. S., Zhu, R., Liu, Z., Lu, L., Peng, J., Tang, Z., Lo, C. H., & Chan, W. K. (2016). Estimation of Hong Kong's solar energy potential using GIS and remote sensing technologies. *Renewable Energy, 99*, 325–335.
Wouters, C., Fraga, E. S., & James, A. M. (2015). An energy integrated, multi-microgrid, MILP (mixed-integer linear programming) approach for residential distributed energy system planning – a South Australian case-study. *Energy, 85*, 30–44.

Yang, Y., Zhang, S., & Xiao, Y. (2015). An MILP (mixed integer linear programming) model for optimal design of district-scale distributed energy resource systems. *Energy, 90*, 1901–1915.
Yao, X., Fan, Y., Zhao, F., & Ma, S. C. (2022). Economic and climate benefits of vehicle-to-grid for low-carbon transitions of power systems: a case study of China's 2030 renewable energy target. *Journal of Cleaner Production, 330*, 129833.
You, L., Tuncer, B., Zhu, R., Xing, H., & Yuen, C. (2019). A Synergetic Orchestration of Objects, Data, and Services to Enable Smart Cities. *IEEE Internet of Things Journal*, *6*(6), 10496–10507.
Yu, R., Zhong, W., Xie, S., Yuen, C., Gjessing, S., & Zhang, Y. (2016). Balancing power demand through EV mobility in vehicle-to-grid mobile energy networks. *IEEE Transactions on Industrial Informatics, 12*(1), 79–90.
Zhang, Y., Qin, W., Wang, L., Yang, C., Su, X., & Wu, J. (2023). Enhancement of Photovoltaic power potential in China from 2010 to 2020: the contribution of air pollution control policies. *Remote Sensing, 15*(1), 228.
Zhu, R., Kondor, D., Cheng, C., Zhang, X., Santi, P., Wong, M. S., & Ratti, C. (2022b). Solar photovoltaic generation for charging shared electric scooters. *Applied Energy*, *313*, 118728.
Zhu, R., Kwan, M. P., Perera, A. T. D., Fan, H., Yang, B., Chen, B., Chen, M., Qian, Z., Zhang, H., Zhang, X., Yang, J., Santi, P., Ratti, C., Li, W., & Yan, J. (2023). GIScience can facilitate the development of solar cities for energy transition. *Advances in Applied Energy*, *10*, 100129.
Zhu, R., Wong, M. S., Kwan, M. P., Chen, M., Santi, P., & Ratti, C. (2022a). An economically feasible optimization of photovoltaic provision using real electricity demand: a case study in New York City. *Sustainable Cities and Society, 78*, 103614.
Zhu, R., Wong, M. S., You, L., Santi, P., Nichol, J., Ho, H. C., Lu, L., & Ratti, C. (2020). The effect of urban morphology on the solar capacity of three-dimensional cities. *Renewable Energy*, *153*, 1111–1126.
Zhu, R., You, L., Santi, P., Wong, M. S., & Ratti, C. (2019). Solar accessibility in developing cities: a case study in Kowloon East. Hong Kong. *Sustainable Cities and Society*, *51*, 101738.

Publisher's Note